Perspective – Synthetic DEMs: A vital underpinning for the quantitative future of landform analysis?

J. K. Hillier[1], G. Sofia[2], and S. J. Conway[3,4],

[1]{Dept. Geography, Loughborough University, United Kingdom, LE113TU}

[2]{Dept. Land, Environment, Agriculture and Forestry, University of Padova, Agripolis, viale dell'Università 16, 35020 Legnaro (PD), Italy.}

[3]{Dept. Physical Sciences, The Open University, Milton Keynes, MK7 6AA, UK}

[4] now at {Laboratoire de Planétologie et Géodynamique de Nantes, Université de Nantes, 2 rue de la Houssinière, 44300 Cedex 3 France}

Correspondence to: J. K. Hillier (jkhillier@lboro.ac.uk)

Abstract

Physical processes, including anthropogenic feedbacks, sculpt planetary surfaces (e.g., Earth's). A fundamental tenet of Geomorphology is that the shapes created, when combined with other measurements, can be used to understand those processes. Artificial or synthetic Digital Elevation Models (DEMs) might be vital in progressing further with this endeavour in two ways. First, synthetic DEMs can be built (e.g., by directly using governing equations) to encapsulate the processes, making predictions from theory. A second, arguably under-utilised, role is to perform checks on accuracy and robustness that we dub 'synthetic tests'. Specifically, synthetic DEMs can contain *a priori* known, idealised morphologies that numerical landscape evolution models, DEM-analysis algorithms, and even manual mapping can be assessed against. Some such tests, for instance examining inaccuracies caused by noise, are moderately commonly employed whilst others are much less so. Derived morphological properties, including metrics and mapping (manual and automated) are required to establish whether or not conceptual models represent reality well, but at present their quality is typically weakly constrained (e.g., by mapper inter-comparison). Relatively rare examples illustrate how synthetic tests can make strong 'absolute' statements about landform detection and quantification; e.g., 84% of valley heads in the real landscape are identified correctly. From our perspective, it is vital to verify such statistics quantifying the properties of landscapes as ultimately this is the link between physics-driven models of processes

and morphological observations that allows quantitative hypotheses to be tested. As such the additional rigor possible with this second usage of synthetic DEMs feeds directly into a problem central to the validity of much of geomorphology. Thus, this note introduces synthetic tests and DEMs, then it outlines a typology of synthetic DEMs along with their benefits, challenges and future potential to provide constraints and insights. The aim is to discuss how we best proceed with uncertainty-aware landscape analysis to examine physical processes.

1 Introduction

Physical processes sculpt planetary surfaces such as the Earth's. A fundamental tenet of Geomorphology is that the form of the surface created, when combined with other data or modelling, can be used to understand those processes. This endeavour to reconcile observation and theory is, essentially, model validation [e.g., Martin and Church, 2004; Pretty, 2009; 2010] summarized by the question: Has the right model been constructed? [Balci, 1998]. Fig. 1 illustrates the pathways towards reconciliation between observations and models, which in geomorphology is conducted through some properties or metrics diagnostic of the landscape of interest; the pathways lead to this reckoning from both physical reality and from conceptual models, which may vary in sophistication (e.g., may even be qualitative). Whilst visual comparisons of landscape properties are obviously possible, quantitative morphometrics of DEMs ('observe' in Fig. 1) are a stronger approach and these vary according to the types of study being undertaken.

Discrete landforms [cf. Evans, 2012] (e.g., craters, cirques, drumlins, volcanoes) can be delimited with a closed boundary and then isolated in order to quantify key characteristics such as height *H* or slope of a flank [e.g., Hillier, 2008]. Linear features (e.g., rivers) can also be measured. Equally, spatially continuous properties of Digital Elevation Models (DEMs) can be quantified (e.g., roughness, Wetness Index) [Beven and Kirkby, 1979; Grohmann et al., 2011; Eisank et al. 2014]. Such morphology-derived observational data, including metrics from mapping that is both manual and automated, add to the more qualitative assessments that may be drawn directly from geomorphological maps.

Quantifying discrete landforms can give additional insights and provide constraints on models of physical processes. For example, discrete fluvial bedforms and their variability are quantified and used to predict extremes for engineering purposes (e.g., depth to place a pipeline) [van der Mark et al., 2008]. Impact crater size-frequency distributions are used to estimate the age of the surface of the Moon and planetary bodies (e.g., Mars and Mercury) [e.g., Hartmann and Neukum, 2001; Ivanov, 2002]. Similarly, size-frequency distributions of volcanoes have been used to examine how melt penetrates the tectonic plates [e.g., Wessel, 2001; Hillier and Watts, 2007]. Aeolian dune formation can be constrained by their sizes [e.g., Duran, 2011; Bo et al., 2011]. In sub-glacial geomorphology 'flow-sets' of proximal bedforms thought to created by the same ice motion occur exponentially less often as their size increases (Fig. 2), which

arguably indicates that substantive elements of the ice-sediment-water system beneath ice sheets contain randomness [Hillier et al., 2013].

Quantitative analysis can also provide constraints when applied to linear features and spatially continuous measures. Channel geometry is measured to investigate the influences of tectonic or climatic landscape forcing [e.g., Brummer and Montgomery, 2003; Wohl, 2004; Sofia et al., 2015], and channel networks are identified to evaluate hydrological responses in floodplains [e.g., Cazorzi et al. 2013]. Continuous measures such as curvature can arguably distinguish dominant geomorphic processes (e.g., diffusive vs fluvial) [e.g., Tarolli and Dalla Fontana, 2009; Lashermes et al., 2007], and can be designed to detect the presence of anthropogenic features (e.g., agricultural terraces) [Sofia, et al., 2014]. They can also be used to estimate the probability of landsliding during rainstorms or for (semi-)automated geomorhological mapping [e.g., Tarolli and Tarboton, 2006; Milledge et al., 2009; Eisank et al., 2014]. Thus, such quantifications also have value for geomorphic understanding. Importantly, these examples illustrate how a robust, reproducible and quantitative approach can be used to develop our understanding of process.

Any enhanced use of landform observations, however, relies on us being able to trust what we have mapped or quantified. Specifically, the key question is; in terms of precision, accuracy and mapping completeness to what extent is it possible to trust the metrics derived from morphometric quantification of the landforms or surface recorded in the DEMs?

One way around this difficulty is to derive descriptive statistics that are as robust as possible to observational shortcomings [e.g., Hillier et al., 2013; Sofia et al, 2013; Tseng et al., 2015]. Another solution is to assess the quality of the morphological mapping and quantification, perhaps either by an estimate of data completeness or quality [e.g., Hillier & Watts, 2007] or by traditional inter-comparisons between mappers [e.g., Podwysocki et al, 1975; Siegal, 1977; Smith and Clark, 2005] or techniques [e.g., Sithole et al., 2004]. The difficulty with robust statistics is that they will still be distorted if shortcomings are substantial [e.g., Hillier and Watts, 2004], and inter-comparisons can only ever yield relative levels of success and even complete agreement is inconclusive; all techniques, mappers, or techniques calibrated to mappers [e.g., Robb et al., 2015] may be systematically missing things (e.g., smaller features [Eisank et al., 2014; Hillier et al., 2014]). Furthermore, it is simply not possible to calculate or estimate the magnitude of potential systematic biases within these approaches. An alternative is to verify each method or result against suitable features or properties known *a priori* within

a suitably constructed test DEM. Thus designed landscapes, or ‘synthetic’ DEMs, can give strong ‘absolute’ answers (e.g., 84% of valley heads in the real landscape are identified correctly), and may be vital in allowing us to proceed better with uncertainty-aware landscape analysis to examine physical processes.

Synthetic DEMs built by directly using postulated governing equations that encapsulate processes, or Landscape Evolution Models (LEMs) [e.g., Chase, 1992], are another key part of examining the form-process link. By altering their constants (e.g., rainfall, hillslope diffusivity) and mathematical construction they can give insights into the drivers and impacts of physical processes [e.g., Willgoose et al., 1991; Montgomery and Dietrich, 1994; Miyamoto and Sasaki, 1997]. LEMs are, however, not yet the whole solution since to be securely compared to reality equivalent landforms within both DEM types must still be robustly quantified, sometimes making validation or calibration very difficult [e.g., Martin and Church, 2004; DeLong et al., 2007]. It is also possible to use synthetic DEMs to test for inaccuracies in DEMs created by LEMs or by measuring a landscape (i.e., 'make' in Fig. 1); one example of this might be requiring that LEMs replicate analytic solutions of the governing equations for simple geometries and forcings. Ultimately, all synthetic DEMs originate in a conceptual view of at least one aspect of a landscape (e.g., drumlin shape, stream-power based fluvial behaviour).

This note introduces synthetic tests and DEMs, then it outlines a typology of synthetic DEMs along with their benefits, challenges and future potential to provide constraints and insights. Note that ‘virtual’ and ‘artificial’ are used interchangeably with ‘synthetic’, as they are in the literature.

2 Synthetic Tests and the Potential Uses of Synthetic DEMs

In fields such as geophysics it is standard to verify any method against its performance on some idealised or ‘synthetic’ data. A well-documented example is the classic ‘synthetic checkerboard’ test [e.g., Dziewonski et al., 1977, Saygin and Kennett, 2010] used in tomographic imaging of the Earth’s interior. Broadly, there are four requisite stages for such a test based upon synthetic data [e.g., Nolet et al., 2007].

1. *Construct a synthetic input* including any features of interest (e.g., the morphology of a landform).

2. *Create the synthetic data* that resembles the observed data, for instance adding suitable noise.
3. *Invert the synthetic data* using the same numerical approach applied to the observed data.
4. *Compare the inverted result with the synthetic input* to see how well the assumed synthetic input (e.g., landform) is recovered.

The difficulty always lies in generating a suitable, statistically representative synthetic; in the case of geomorphology the task is to create an 'appropriate' synthetic landscape or DEM that is realistic enough in the aspects under investigation.

DEMs containing a synthetic component have been employed in 'synthetic tests' to assess approaches used to estimate the fractal dimension of topography [Malinverno, 1989; Rodriguez-Iturbe and Rinaldo, 1997; Tate, 1998a,b], slope and aspect [Zhou, 2004], land surface parameters (LSPs) [e.g., Wechsler, 2006; Sofia et al, 2013], and the reliability of DEMs [e.g., Fischer, 1998; Oksanen, 2010]. Additionally, they have been used to evaluate how well some features (e.g., river networks, terraces) are identified [Pelletier, 2013; Sofia et al., 2014] and others (e.g., submarine volcanoes and drumlins) are isolated in 3D (i.e., their volumes explicitly delimited) [Wessel, 1998; Hillier, 2008; Kim and Wessel, 2008; Hillier & Smith, 2014]. Synthetics have also been used to assess algorithms quantifying landscape processes such as flow-routing [e.g., Pelletier, 2010] and to give a first insight into how effective the manual mapping of glacial bedforms is [Hillier et al., 2014]. Often, when including randomness (e.g., in locations or noise) in a *Monte Carlo* approach multiple realisations of a landscape (e.g., n = 10 or 1,000) are used to understand uncertainty and variability and more tightly constrain results [e.g., Heuvenlink, 1998; Raaflaub and Collins, 2006; Wechsler, 2006]. The large (e.g., 60-66% in Hillier et al. [2014]) and systematic trends and biases that studies so far have uncovered indicates that the uses of synthetic tests in geomorphology should be, arguably, similar in extent and function to the current use of inferential statistics; namely they are a demonstration that the observation claimed actually exists or method actually works. Some potential applications of synthetic tests in geomorphology can be categorised as:

- Assessing the impact of 'noise' [e.g., Sofia et al., 2013; Zhou and Liu, 2002, 2008] that could be instrumental, anthropogenic (e.g., houses) or natural (e.g.,

vegetation). This applies to making DEMs from measurement, and making quantitative observations from any DEM.

- When observing, verifying that a geomorphic signature is actually characteristic of a particular landform type of interest, rather than other morphologies in a study area [e.g., Conway et al., 2011; Sofia et al., 2014].
- Quantifying extraction of features using metrics such as completeness, reliability [e.g., Hillier et al., 2014; Eisank et al., 2014]; in this the key advantage is that synthetics give ‘absolute’ measures of accuracy simply not possible with traditional mapper inter-comparisons (e.g., 34-40% of drumlins can be detected).
- Assessing filtering or other techniques used to manipulate a DEM [e.g., Hillier & Smith, 2014], whose choice would otherwise be subjective.
- Evaluating the sensitivity of algorithms quantifying geomorphic processes to modelling assumptions, such as DEM resolution [e.g., Pelletier, 2010].
- Determining whether or not LEMs have been correctly constructed (i.e. 'make' in Fig. 1).

Ultimately, the geomorphological intention is to use synthetic DEMs to examine more clearly the expression of physical processes. Rigor added to geomorphological observations through testing with synthetic DEMs will, we believe, ultimately link physics-driven models of processes to morphological observations, allowing quantitative hypotheses to be formulated and tested [e.g., see McCoy, 2015]. This is illustrated in Fig. 1, the crux of which is that it is necessary to quantify landscape properties to rigorously reconcile DEMs, with some main elements of this described in more detail below.

If arguably realistic forms can be generated directly by a physics-based model [e.g., Dunlop et al., 2008; Refince et al., 2012; Brown, 2015] creating a synthetic DEM, these may in principle be linked directly to reality if suitably equivalent field sites can be found, measured, and recorded in a DEM. The effects of various constants (e.g., rainfall), conditions and processes in the physical models on observables can be viewed and compared to reality by the simple expedient of turning them off or amplifying them, of course allowing carefully for appropriate initial and boundary conditions. Comparisons have been qualitative [e.g., Kaufman, 2001], but can provide more powerful insights if they apply consistent mapping or quantification procedures [e.g., Willgoose et al., 1994]. Thus, creating a form-process link will still depend critically upon understanding any errors or biases in landform morphometrics (e.g., in size-frequency distributions, dominant wavelength) for both the measured and generated landscapes (i.e., 'observe'

in Fig. 1). The appropriate metrics are better understood for some landforms than for others, and it is only possible to adequately assess their efficacy (i.e. in an absolute sense) with tests involving *a priori* information and a DEM to apply the morphometric extraction method to, or by our definition using a synthetic DEM. If laboratory experiment replaces LEM-derived synthetic DEMs in the paragraph above, the same logic applies.

For a landform that it is not yet possible to create numerically from first mathematical principles, other routes exist. The challenge is to securely relate the driving process (e.g., tectonic uplift rate) to a measure of morphology (i.e., 'conceptual model' to 'landscape properties' on Fig. 1), perhaps using its variability within geographical areas. For example, drumlin sizes observed for a number of flow-sets might be compared to characteristics of flow within a modelled ice sheet (e.g., flow velocity) representative of the area of the flow-set. Statistical models can be formulated that link size-frequency observations to parameters in numerical ice-flow models [Hillier et al., *in review*], but even potential empirical rules about timing (e.g., immediately before de-glaciation) and the relationships to ice flow (e.g., size directly proportional to velocity) could be tested. Robustly determined observational metrics would be needed for such an inversion; i.e., synthetic tests are needed. Realistic models are likely to contain stochastic elements [e.g., Tucker et al, 2001], thus a statistical understanding may help to identity more effectively appropriate parameterizations for size observations (e.g., Weibull) than testing a variety of established distributions [e.g., van der Mark, 2008]. Observational robustness is desirable in this case, but also for approaches that make predictions about landscape properties directly from conceptual models, for instance dominant wavelengths [e.g., Anderson, 1953; Venditti, 2013].

A final use of synthetic DEMs is examining ‘what if’ engineering scenarios as they affect behaviours such as hydrological processes [e.g., Tarolli et al., 2015]. This may be somewhat tangential, but imposing a proposed artificial geometry onto a measured DEM as a way of testing an artificial geometry to be created on the part of the Earth’s surface is clearly a legitimate pursuit.

3 Synthetic DEM Typology

Synthetic DEMs are only useful if they can be constructed, and their construction must be from or clearly identify ‘components’ (e.g., a landforms layer). In contrast to viewing a landscape as plan-view regions, height in DEMs can be described at any location (x, y)

as the sum of *n* 'components' (Eq. 1) [e.g., Wren, 1973; Wessel, 1998; Hillier and Smith, 2008], namely $H_{DEM} = H_1 + H_2 + \ldots\ldots H_n$. Conceptually, these components lie on top of each other, like geological strata, and extend across the entire DEM although they may have zero thickness for few or many parts of it.

For landform analysis the first component would typically be 'noise' (e.g., DEM error, or surface 'clutter' such as trees), the small-scale height variations not genetically related to the landform. A second component would be the landforms themselves, perhaps overlying a third component of larger-scale trends (e.g., 10 km wide smoothly undulating hills). However, in the limit, only one component is actually required, and how the components are constructed will vary depending upon the purpose of the synthetic DEM. Furthermore, the synthetic DEM might mix idealised, created components with real ones. Typically randomness is involved in the creation of statistical synthetics, and multiple realisations of landscapes may be created. The broad approaches to constructing synthetic DEMs are outlined in the typology below.

3.1 Simple and Statistical

Perhaps the simplest synthetic DEMs are those constructed by using basic geometries as building blocks such as cones, Gaussian functions, and planes or other surfaces defined by simple equations [e.g., Hodgson, 1995; Wessel, 1997; Jones, 1998; Kim and Wessel, 1998; Hillier, 2008; Pelletier, 2010; Qin et al., 2012]; admittedly, some functions may be less simple [e.g., Pelletier, 2013; Minár et al., 2013]. Typically, generalized shapes (e.g., 2D Gaussian, rotated parabola) are formulated based upon visual or statistical fitting of the functions to measured morphologies [e.g., Conway et al., 2011; Hillier and Smith, 2012; Pelletier, 2013] (Fig. 3); fits may not be perfect (Fig. 3b), highlighting that all synthetic DEMs are simplifications of reality.

These synthetics do not contain the complexity in the observed landscape, or necessarily have realistic statistical properties, but they have the advantages of being simple to construct and understand, and noise can be entirely omitted or modified with certainty in order to investigate data errors. They contain the key morphologies under investigation and are perfectly sufficient for some tests; e.g., are approximately conical submarine volcanoes of variable size effectively isolated even when upon a slope? (Fig. 4). Statistically generated 'noise' can be added to simple synthetic DEMs to assess the degradation caused [e.g., Zhou, 2004; Jordan and Watts, 2005], but for results to be meaningful its statistical distribution (e.g., Gaussian, uniform), length-scale of correlation, and any non-stationarity must be correct [e.g., Fischer, 1998, Sofia et al., 2013].

Whole landscapes can be generated statistically using fractals [e.g. Mandelbrot, 1983] or multi-fractals (Fig. 5a) [e.g., Gilbert, 1989; Schertzer and Lovejoy, 1989; Weissel, 1994; Cheng, 1996], and these can be useful if the construction matches closely the element of reality being considered (e.g., uncorrelated, fractal in Swain and Kirby [2003]). Even multi-fractal landscapes, however, may not be an adequate representation without considering properties such as anisotropy [e.g., Evans and McClean, 1995; Gagon, 2006] and characteristic scales [e.g., Perron, 2008] if they are important in a particular circumstance. A limitation of these purely statistically generated, or statistically altered, DEMs for landform analysis is that they do not explicitly contain spatially distinct, isolated features (i.e., landforms are not labelled as such during generation).

3.2 Landscape Evolution Models

DEMs resembling real landscapes can also be created by the application of mathematical characterisations of physical processes in numerical models typically known as 'Landscape Evolution Models' (LEMs) (Fig. 5b) [e.g., Chase, 1992; Braun and Sambridge, 1997]; implementation approaches can vary [see Griffin, 1987]. These now incorporate numerous processes [e.g., Tucker, 2010; Refice et al., 2012]; for example, bedrock landslides [e.g., Densmore, 1998], flexure of the lithosphere [e.g. Lane et al., 2008], and erosion by ice flow within valleys [e.g. Harbor, 1992; Brocklehurst and Wipple, 2004; Amundson and Iverson, 2006; Tomkin, 2009], including when this is thermo-mechanically coupled to ice sheets [e.g. Jamieson et al., 2008]. Models of the evolution of single classes of feature (e.g., bedforms) and simpler 2D configurations (i.e., x-z profiles) fall within this class of model [cf. Dunlop et al., 2008; Zhang et al., 2010; Brown et al., 2014]. Simple geometries or measured landscapes may be used as an input [e.g., DeLong et al., 2007; Refice et al., 2012; Baartman et al., 2015; Hancock et al., 2015].

Several difficulties prevent these models from, as yet, being ideal solutions. In terms of testing observational methods, the first difficulty is that the method of generating some landforms such as drumlins from first principles is often contested [cf., Hindmarsh, 1998; Schoof, 2007; Pelletier, 2008], and it is not computationally practical to include certain processes, such as impact crater formation in the MARSSIM model [Howard, 2007]. The simulation of rivers illustrates an area where there is progress, but also much to do [cf. Coulthard et al., 2013; Brown et al., 2014]. In general, a highly accurate and widely accepted unified model is still some way off. The second difficulty is that these models do not currently associate processes with a type of landform. For

instance, a bedrock failure process is a bedrock failure process, not a bedrock failure process explicitly making a V-shaped valley. Equally, sediment is not tagged as making a floodplain. So, the number and location of defined features are not known *a priori*. This can be seen as a strength of the models, but means that creating a secure link from process to landforms as observed in reality requires a step in which consistent mapping or quantification procedures are applied to both measured and simulated DEMs. This is not easy [e.g., DeLong, 2007]. The lack of *a priori* features may also be the reason that, although LEMs have great potential to create DEMs for synthetic tests of landform mapping or extraction methodologies, we are not aware of this being done. Like simple or statistical synthetic DEMs, synthetics created by a LEM have the advantage of being free from errors associated with DEM measurement (e.g., instrumental, processing).

3.3 Laboratory derived

If LEM-derived DEMs can be considered as synthetic DEMs, then laboratory-derived ones [e.g., Hancock and Willgoose, 2001; Lauge et al. 2003; Graveleau and Dominguez, 2008; Sweeny et al. 2015] could also be considered so. Such experiments can control variables such as rainfall and uplift that are impossible to precisely control in nature [e.g. Sweeny et al 2015], but limitations in realism exist particularly in scaling [see Paola et al., 2009].

3.4 Complex geometrical

A possible class of synthetic DEM is one that uses simple or statistical building blocks, but constructed in a more complex fashion. For instance, multiple idealised shapes can be given additional observed attributes (e.g., spatial clustering, size-frequency realism) [e.g., Howard, 2007; Hillier and Smith, 2012], but such DEMs have so far contained other elements of realism as well, perhaps making them better described as hybrids.

3.5 Hybrid

A 'hybrid' class of synthetic DEM contains, for reasons of practicality, elements of the other classes. Typically, a morphology whose key properties cannot currently be readily simulated is either retained (e.g., most or all of a measured DEM), or an idealised but observationally constrained component is added (e.g., terraces [Sofia et al. 2014]), or both. The spectrum of what is possible is illustrated by the, relatively rare, studies using hybrid synthetic DEMs in geomorphology.

A first example of a hybrid synthetic DEM is impact crater formation in the MARSSIM model [Howard, 2007]. This evolution model does not dynamically model crater

348 formation. Instead, randomly located craters are assigned shapes from a catalogue of
349 measurements of individual fresh craters on Mars and given sizes from a power-law
350 distribution. This introduces certain assumptions, such as the fresh craters being
351 representative, but avoids complexity. A second example deals with the quantification of
352 glacial bedforms, illustrated with drumlins [Hillier and Smith, 2012; Hillier and Smith,
353 2014; Hillier et al, 2014]. It is the association of the bedforms with underlying trends
354 (i.e., 'hills') and complex and spatially structured 'noise' (e.g., trees, roads, houses) that
355 makes the quantification difficult; in particular, this noise is problematic, and
356 geomorphological analyses have yet to attempt simulating it. The approach taken was
357 therefore to circumvent this issue entirely by leaving the hills and noise as they were,
358 and moving the drumlins such that they were randomly positioned with respect to these
359 problems for identification (Fig. 6). Orientations and spatial density distribution (i.e.,
360 number per km^2) were preserved, as were the geometries (i.e., height-width-length
361 triplets) of the 173 drumlins shuffled around. In these synthetics (Fig. 7), the number
362 and location of defined features are known *a priori* such that sizes and locations of
363 mapped discrete landforms can be compared to synthetic ones directly. Similarly, but by
364 assuming the highest-quality measured LiDAR DEMs were perfect, even if this is
365 debatable, it is possible to circumvent the need to generate statistically realistic
366 landscapes when investigating DEM errors [Raaflaub and Collins, 2006; Sofia et al.,
367 2013]. Anthropogenic elements (e.g., open-cast mines, terraces) visually determined to
368 be reasonable can also be added [e.g., Baartman et al., 2015], for instance to a 2D
369 multi-fractal statistical landscape [Sofia et al., 2104; Chen et al. 2015].

370

371 **4 Discussion**

372 By providing an *a priori* known answer to test against, synthetic DEMs or DEMs
373 containing a synthetic component have some clear and powerful advantages in
374 geomorphological analyses. They can be used to test errors, systematic or random
375 biases, and unpick potential sources of misinterpretation. Furthermore, they give
376 *absolute* answers (e.g., 47% of all actual drumlins $H > 3$ m are mapped) to questions
377 about accuracy that are simply not obtainable by other means, and are often considered
378 'objective'. Through this they provide a route to answering key questions about
379 geomorphic processes (e.g., Fig. 1). There are, however, complexities surrounding
380 these statements, which are less commonly recognised. There are issues of objectivity,
381 realism, circularity and the cost in time and effort of constructing synthetics.

Whilst the conclusions reached through the use of synthetics may be simplistically thought of as objective, it is more accurate to say that they are quantitative, reproducible, and are likely to be significantly less subjective. Without perfect, all-purpose synthetics an element of subjectivity will remain in the choices made when designing the test DEM. Hillier and Smith [2012] illustrate some choices and a logical justification for them. Manually selecting data to test against [e.g., Sithole, 2004; Hillier & Watts, 2004] is faster in some circumstances, if more subjective. Reproducibility makes testing using synthetic DEMs superior to subjective visual verification, even if synthetic tests later indicate the visual estimate was a reasonable solution [Hillier and Smith, 2012, 2014]. Pre-existing synthetic DEMs, however, are entirely objective means for inter-comparison for future studies [e.g., Eisank et al., 2014].

A thorny question regarding synthetics is: how realistic is realistic enough? At one limit, it is notable that even extreme simplifications such as conical volcanoes can give significant and useful first-order insights [e.g., Kim and Wessel, 2008; Tarolli et al, 2015]. At the other limit, synthetic DEMs are not used on the basis that their applicability to real datasets is questioned [e.g., Robb et al., 2015]. Lacking a perfect set of properties, however, should not be taken to invalidate tests using a synthetic DEM; in statistics for instance, Student's t-test underpinned by its idealized Gaussian distribution is widely used although observations are rarely perfectly Normal. A challenge then is to determine a generalised objective framework or workflow to assess the sufficiency of the realism of synthetic DEMs, but in its absence what can be done? Deficiencies can be visually identified. For instance, if spatial resolution is raised as an issue, it can either be matched to the observed data, or varied for a sensitivity test. If a particular statistical property and its variation with scale is key, it can be measured to ensure it is realistic in the synthetic. So, if a clearly stated set of properties argued to be most relevant to any given research task are faithfully reproduced in synthetics, we believe they will provide useful insights. Ultimately, however, practitioners within a peer-group must decide what is convincing, performing additional tests if necessary. For example, Hillier and Smith [2012] did not locally align neighbouring drumlins with each other, but participants the GMapping workshop [Hillier et al., 2014] felt that this was critical. Modified DEMs with this property included were therefore provided, although in the end this proved to be a minor effect. Similarly, what must be captured well in a synthetic DEM may critically vary between studies. This is exemplified by the impact of life (e.g., buildings, earthworks, trees, eco-geomorphic work by worms), which may either be inconvenient

'noise' [e.g., Hillier & Smith, 2012] or the morphology of interest [e.g., Dietrich and Perron, 2006].

A more subtle potential issue is circularity. It is important to avoid basing aspects of a synthetic DEM on an assumption, and then using it to support the assumption. This is easily avoided in simple synthetic DEMs but a synthetic DEM based on a landscape evolution model, for instance, should not later be justified because a search algorithm trained on it finds only similar features in a real landscape; the algorithm might just be missing things in the real landscape that differ from what it has been trained to detect. A similar issue was faced by Hillier and Smith [2012], but demonstrably avoided as the filter later found to be optimal was not the one initially assumed [Hillier and Smith, 2014].

So, subjectivity is reduced, even synthetic tests using basic DEMs can give some insight, and circularity can be avoided. On balance we argue that, if designed appropriately and used with appropriate care, tests using synthetic DEMs are worth the cost in time as they can be used to access results and insights of real significance and power. Exactly the same can be said for the application of statistical techniques, and so it seems reasonable to advocate the use of synthetic tests with similar strength.

By making observations more robust synthetic tests using synthetic DEMs containing *a priori* known landforms have the potential to strengthen the insights that can be gained through synthetic DEMs generated using physics-based numerical models, i.e. Landscape evolution models. LEMs can provide useful insights, but they are not the entire solution; firstly, they cannot model all processes yet, and secondly they are insufficient without synthetic tests to secure the observational part of the linkage between measured and generated DEMs. It is also worth noting that landscape evolution models are not the only route to creating a from-process link since the other routes described (e.g., statistical) also provide a quantitative means of establishing a form-process link even without a LEM. Thus, there are a number of valid types and specific uses of synthetic DEMs, but in combination we believe that they form a vital underpinning for the quantitative future of landform analysis [e.g., see McCoy, 2015].

5 Conclusions

From this discussion on the uses of synthetic digital landscapes (i.e., DEMs), or synthetic elements within them, the following overarching points can be drawn:

- Synthetic DEMs can help to link physics-based models of processes to morphological observations, allowing quantitative hypotheses to be formulated and tested; importantly, this is not only through the use of landscape evolution models.
- By establishing 'absolute' answers tests using synthetic DEMs containing *a priori* known landforms are a powerful tool with which to test and add rigor to geomorphological observations, and arguably should become as standard as statistical tests in geomorphology or synthetic test data in other arenas (e.g., Geophysics).
- A 'perfect' synthetic DEM faithfully representing all aspects of an environment is likely impractical or impossible to create at present, but is not necessary.
- Synthetic DEMs for tests may be easy and simple to construct, yet still provide valuable insights.
- Synthetic tests using DEM's should be tailored to each research question, and their appropriateness to the key aspects of each inquiry (e.g., resolution, biases, and sensitivities) set out clearly and logically.

Acknowledgements

LiDAR data in Fig. 5c were provided by the Italian Ministry for Environment, Land and Sea (Ministero dell'Ambiente e della Tutela del Territorio e del Mare, MATTM), as part of the PST-A framework. The GMT software were used [Wessel and Smith, 1998]. SJC was funded by a Leverhulme Trust Grant RPG-397. We thank J. Pelletier, I. Evans and an anonymous reviewer for their fair and insightful comments.

References

Amundson, J. M., Iverson, N. R., 2006. Testing a glacial erosion rule using hang heights of hanging valleys, Jasper National Park, Alberta, Canada. *J. Geophys. Res. Earth* Surface 111, art. no. F01020.

Anderson, A.G., 1953. The characteristics of sediment waves formed on open channels. *Proceedings of the Third Mid-Western Conference on Fluid Mechanics*. University of Missouri, Missoula, 397–395.

Baartman, J. E. M., Masselink, R., Keesstra, S. D. and Temme, A. J. A. M., 2013. Linking landscape morphological complexity and sediment connectivity. *Earth Surf. Process. Landforms*, **38**: 1457–1471. doi: 10.1002/esp.3434.

Balci, O. Verification, Validation, and Testing, in Banks. J. (Ed.), *Handbook of Simulation: Principles, Advances, Applications, and Practice*. Wiley, 335-393.

Beven, K. J., Kirkby, M. J., 1979. A physically based variable contributing area model of basin hydrology, *Hydrol. Sci. Bull.*, **24**(1), 43–69.

Braun, J., Sambridge, M, 1997. Modelling landscape evolution on ge ological time scales: A new method based on irregular spatial discretization. *Basin Research* **9**, 27-52.

Brocklehurst, S. H., Wipple, K. X., 2004. Hypsometry of glaciated landscapes. *Earth Surface Processes and Landforms* **29**, 907-926.

Brown, R. A., Pasternack, G. B. & Wallender, W. W., 2014. Synthetic river valleys: Creating prescribed topography for form–process inquiry and river rehabilitation design. *Geomorphology* **214**, 40–55.

Brummer, C.J., Montgomery, D.R., 2003. Downstream coarsening in headwater channels. *Water Resour. Res.* **39**(10). doi:10.1029/2003WR001981

Cazorzi, F., Dalla Fontana, G., De Luca, A., Sofia, G., Tarolli, P., 2013. Drainage network detection and assessment of network storage capacity in agrarian landscape. *Hydrol. Process.* **27**(4), 541-553. doi:10.1002/hyp.9224

Chase, C. G., 1992. Fluvial landscupting and the fractal dimension of topography. *Geomorphology* **5**, 39-57.

Chen, J., Li, L., Chang, K., Sofia, G., Tarolli, P., 2015. Open-pit mining geomorphic feature characterization. *International Journal of Applied Earth Observation and Geoinformation*, 42, 76-86, ISSN 0303-2434, http://dx.doi.org/10.1016/j.jag.2015.05.001

Cheng, Q. M., Agterberg, F. P., 1996. Multi-fractal modelling and spatial statistics *Mathematical Geology* **28**, 1-16.

Clark, C. D., Hughes, A. L. C., Greenwood, S. L., Spagnolo, M., Ng, F. S. L., 2009. Size and shape characteristics of drumlins, derived from a large sample, and associated scaling laws, *Quat. Sci. Rev.*, **28**(7-8), 677–692, doi:10.1016/j.quascirev.2008.08.035.

525 Conway, S. J., Balme, M. R., Murray, J., Towner, M. C., Okubo, C. H., Grindrod, P. M.
526 2011. The indication of Martian gully formation processes by slope–area analysis, *Geol.*
527 *Soc. Spec. Publ*., **356**, 171–201, doi:10.1144/SP356.10.
528
529 Coulthard, T.J., Neal, J.C., Bates, P.D., Ramirez, J., de Almeida, G.A.M., Hancock,
530 G.R., 2013. Integrating the LISFLOOF-FP 2D hydrodynamic model with the CAESAR
531 model: implications for modelling landscape evolution. *Earth Surf. Process. Landf.*
532 http://dx. doi.org/10.1002/esp.3478.
533
534 Densmore, A. L., Ellis, M. A., Anderson, R. S., 1998. Landsliding and the evolution of
535 normal-fault-bounded mountains. *J. Geophys. Res.* **103**(B7), 15203-15219.
536 doi:10.1029/98JB00510
537
538 Dietrich, W.E., Perron, J.T., 2006. The search for a topographic signature of life. *Nature*
539 **439**, 411–418.
540
541 Dunlop, P., Clark, C. D. & Hindmarsh, R. C. A., 2008. Bed Ribbing Instability
542 Explanation: Testing a numerical model of ribbed moraine formation arising from
543 coupled flow of ice and subglacial sediment. *J. Geophys. Res.* **113**.
544
545 Dziewonski, A., Hager, B., O'Connell, R., 1977. Large-scale heterogeneities in the
546 lower mantle. *J. Geophys. Res.* **82**, 239-255.
547
548 Eisank, C., Smith, M., Hillier, J. K., 2014. Assessment of multi-resolution segmentation
549 for delimiting drumlins in digital elevation models. *Geomorphology*. **214**, 452-464.
550 doi:10.1016/j.geomorph.2014.02.028.
551
552 Evans, I. S., McClean, C. J., 1995. The land surface is not unifractal; variograms, cirque
553 scale and allometry. Zeitschrift für Geomorphologie, N.F. Supplement-Band 101, 127-
554 147
555
556 Evans, I. S., 2012. Geomorphometry and landform mapping: What is a landform?
557 *Geomorphology*, **137,** 94–106, doi:10.1016/j.geomorph.2010.09.029.
558
559 Fisher P., 1998. Improved modeling of elevation error with geostatistics. *GeoInformatica*
560 **2**, 215–233.
561
562 Gagnon, J. S., Lovejoy, S., Schertzer, D., 2006. Multifractal Earth topography Nonlinear
563 *Processes in Geophysics* **5**, 541-570.
564
565 Gilbert L. E., 1989. Are topographic data sets fractal? *Pure and Applied Geophysics*
566 **131**, 241-254.
567
568 Graveleau, F., Dominguez, S., 2008. Analogue modelling of the interaction between
569 tectonics, erosion and sedimentation in foreland thrust belts. *Comptes Rendus*
570 *Geoscience* **340**, 324–333.
571
572 Grohmann, C., Smith, M. J., Riccomini, C., 2011. Multiscale analysis of surface
573 roughness in the Midland Valley, Scotland. *IEEE Trans. Geosci. Remote Sens.* **49**,
574 1200–1213.
575

576 Hancock, G., Willgoose, G., 2001. Use of a landscape simulator in the validation of the
577 SIBERIA catchment evolution model: Declining equilibrium landforms. *Water Resources*
578 *Research*, **37**(7), 1981-1992.
579
580 Hancock, G., Lowry, J. B. C. & Coulthard, T. J., 2015. Catchment reconstruction —
581 erosional stability at millennial time scales using landscape evolution models.
582 *Geomorphology* **231**, 15–27.
583
584 Harbor, J. M., 1992. Numerical Modeling of the development of U-shaped valleys by
585 glacial erosion. *Geol. Soc. Am. Bull.* **104**,1364-1375.
586
587 Hartmann, W. K., and Neykum, G., 2001. Cratering chronology and the evolution of
588 Mars. *Space Sci. Rev.* **96**, 165–194.
589
590 Heuvelink, G.B.M., 1998. *Error propagation in environmental modelling with GIS*. Taylor
591 & Francis, London, UK.
592
593 Hodgson, M.E., 1995. What cell size does the computerd slope/aspect angle represent?
594 *Photogramm. Eng. Remote Sens.* **61**(5), 513-517.
595
596 Howard, A. D., 2007. Simulating the development of martian highland landscapes
597 through the interaction of impact cratering, fluvial erosion, and variable hydrologic
598 forcing, *Geomorphology*, **91**, 332-363.
599
600 Hillier, J.K., Watts, A.B., 2004. Plate-like subsidence of the East Pacific Rise - South
601 Pacific Superswell system. *J. Geophys. Res.*, **109**, B10102,
602 doi:10.1029/2004JB003041.
603
604 Hillier, J. K., Watts, A. B., 2007. Global distribution of seamounts from ship-track
605 bathymetry data. *Geophys. Res. Lett.* **34** L113304, doi:10.1029/2007GL029874.
606
607 Hillier, J. K., 2008. Seamount detection and isolation with a modified wavelet transform,
608 *Basin Res.*, **20**, 555–573.
609
610 Hillier, J. K., Smith, M., 2008. Residual relief separation: digital elevation model
611 enhancement for geomorphological mapping. *Earth Surface Processes and Landforms*
612 **33**, 2266-2276 doi: 10.1002/esp.1659
613
614 Hillier, J. K., Smith M., 2012. Testing 3D landform quantification methods with synthetic
615 drumlins in a real DEM *Geomorphology* **153** 61-73 doi:10.1016/j.geomorph.2012.02.009
616
617 Hillier, J. K., Smith, M. J., Clark, C. D., Stokes, C. R., Spagnolo M., 2013. Subglacial
618 bedforms reveal an exponential size-frequency distribution, *Geomorphology*,
619 doi:10.1016/j.geomorph.2013.02.017.
620
621 Hillier, J. K. et al., 2014. Manual mapping of drumlins in synthetic landscapes to assess
622 operator effectiveness *J. Maps* doi:10.1080/17445647.2014.957251
623
624 Hillier, J. K., Kougioumtzoglou, I. A., Stokes, C. R., Smith, M. J., Clark, C. D. (*In*
625 *Review*) Stochastic ice-sediment dynamics could explain subglacial bedforms sizes.
626 *PlosONE*.
627

628 Hindmarsh, R. C. A., 1998. Drumlinization and drumlin-forming instabilities: viscous till
629 mechanisms. *J. Glaciology* **44**, 293-314.
630
631 Ivanov, B. A., Neukum, G., Bottke, W. F. & Hartmann, W. K, 2002. The Comparison of
632 Size-Frequency Distributions of Impact Craters and Asteroids and the Planetary
633 Cratering Rate. *Asteroids III* 89–101.
634
635 Jones, K.H., 1998. A comparison of algorithms used to compute hill slope as a property
636 of the DEM. *Comput. Geosci.* **24**, 315–323. doi:http://dx.doi.org/10.1016/S0098-
637 3004(98)00032-6
638
639 Jordan, T. A., Watts, A. B., 2005. Gravity anomalies, flexure and the elastic thickness
640 structure of the India-Eurasia collisional system. *Earth Planet. Sci. Lett.* **236**, 732-750.
641
642 Kim, S. and Wessel. P., 2008. Directional median filtering for the regional-residual
643 separation of bathymetry. *G3* **9**, Q03005 10.1029/2007GC001850
644
645 Lague, D., Crave, A., Davy, P., 2003. Laboratory experiments simulating the
646 geomorphic response to tectonic uplift. *J. Geophys. Res.*, **108**(B1), art. no. 2008.
647
648 Lane, N. F., Watts, A. B., and Farrant, A. R, 2008. An analysis of Cotswold topography:
649 insights into the landscape response to denudational isostasy. *J. Geol. Soc.* **165**, 85-
650 103.
651
652 Lashermes, B., Foufoula-Georgiou, E. & Dietrich, W. E., 2007. Channel network
653 extraction from high resolution topography using wavelets. *J. Geophys. Res.* **34**,
654 L23S04.
655
656 Malinverno, A., 1989. Testing linear models of seafloor topography *Pure and Applied*
657 *Geohpysics* **131**, 139-155.
658
659 Mandelbrot, B., 1983. *The Fractal Geometry Of Nature* W. H. Freeman and Company,
660 New York.
661
662 Martin, Y., Church, M., 2004. Numerical modelling of landscape evolution:
663 geomorphological perspectives. *Progress in Physical Geography*, **28**(3), 317-339.
664
665 McCoy, S., 2015. Landscapes in the lab. *Science*, **349**(6243), 32-33.
666
667 Minár, J., Jenco, M., Evans, I., Minár, J. Jr., Kadlec, M., Krcho, J., Pacina, J., Burian, L.,
668 Benová, 2013. Third-order geomorphometric variables (derivatives): definition,
669 computation and utilization of changes of curvatures. *Int. J. GIS*, **27**(7), 1381-1402.
670
671 Miyamoto, H., Sasaki, S., 1997. Simulating lava flows by an improved cellular
672 automata method. *Computers and Geosciences* **23**, 283–292.
673
674 Montgomery, D.R., Dietrich, W.E., 1994. A physically-based model for topographic
675 control on shallow landsliding. *Water Resources Research* **30** (4), 1153–1171.
676
677 Nolet, G., Allen, R., Zhao, Dapeng, 2007. Mantle plume tomography *Chemical Geology*
678 **241**, 248-263
679

Oksanen J, Sarjakoski T., 2010. Non-stationary modelling and simulation of LIDAR DEM uncertainty. *Proceedings of the 9th International Symposium on Spatial Accuracy Assessment in Natural Resources and Environmental Sciences*, July 20–23, Leicester, UK; 201–204.

Paola, C., Straub, K., Mohrig, D., 2009. The "unreasonable effectiveness" of stratigraphic and geomorphic experiments. *Earth-Science Reviews*, **97**, 1-43.

Pellietier, J. D., 2008. *Quantitative Modelling of Earth Surface Processes*. 185-189. CUP, Cambridge, UK. ISBN 9780521855976.

Pelletier J.D. 2010, Minimizing the grid-resolution dependence of flow-routing algorithms for geomorphic applications, *Geomorphology,* **122** (1–2), 91-98, ISSN 0169-555X, http://dx.doi.org/10.1016/j.geomorph.2010.06.001.

Pelletier, J. D., 2013. A robust, two-parameter method for the extraction of drainage networks from high-resolution digital elevation models (DEMs): Evaluation using synthetic and real-world DEMs, *Water Resour. Res.*, **49**, doi:10.1029/2012WR012452.

Perron, J. T., Kirchner, J.W., Dietrich, W.E., 2008. Spectral signatures of characteristic spatial scales and nonfractal structure of landscapes *J. Geophys. Res.* **113**, F04003.

Petty, M. D., 2009. Verification and Validation, in Sokolowski, J. A. and Banks, C. M. (Eds.), *Principles of Modeling and Simulation: A Multidisciplinary Approach*. Wiley, 121-149.

Petty, M. D. Verification, Validation, and Accreditation, in Sokolowski, J. A. and Banks, C. M. (Eds.), *Modeling and Simulation Fundamentals: Theoretical Underpinnings and Practical Domains*. Wiley, 325-372.

Podwysocki, M.H., Moik, J.G., Shoup, W.C., 1975. Quantification of geologic lineaments by manual and machine processing techniques, *Proceedings of the NASA Earth Resources Survey Symposium*. NASA, Greenbelt, Maryland, pp. 885-905.

Qin, J., Zhong, D., Wang, G., Ng, S. L., 2012. On characterization of the imbrication of armored gravel surfaces. *Geomorphology* **159**, 116–124.

Raaflaub, L.D., Collins, M.J., 2006. The effect of error in gridded digital elevation models on the estimation of topographic parameters. *Environ. Model. Softw*. **21**, 710–732. doi:http://dx.doi.org/10.1016/j.envsoft.2005.02.003

Refice, A, Giachetta, E., Capolongo, D., 2012. SIGNUM: A Matlab, TIN-based landscape evolution model, *Computers & Geosciences* **45**, 293-303, ISSN 0098-3004, http://dx.doi.org/10.1016/j.cageo.2011.11.013.

Robb, C., Willis, I. C., Arnold, N., Gudmundsson, S., 2015. A semi-automated method for mapping glacial geomorphology tested at Breiðamerkurjökull, Iceland. *Remote Sens. Environ.* **163**, 80–90.

Rodriguez-Iturbe, I., Rinaldo, A., 1997. *Fractal river basins: chance and self-organization*. Cambridge University Press. ISBN 0521 47398 5.

Saygin, E., Kennett, B. L. N., 2010. Ambient seismic noise tomography of Australian continent. *Tectonophysics* **481**, 116-125.

Schertzer, D., Lovejoy, S., 1989. Nonlinear Variability in Geophysics: Multifractal Simulations and Analysis, in: Pietronero, L. (Ed.), *Fractals' Physical Origin and Properties* SE - 3, Ettore Majorana International Science Series. Springer US, pp. 49–79. doi:10.1007/978-1-4899-3499-4_3.

Schoof, 2007. Cavitation in deformable glacier beds. *J. Appl. Math.* **67**, 163-1653.

Siegal, B.S., 1977. Significance of operator variation and the angle of illumination in lineament analysis of synoptic images. *Modern Geology* **6**, 75-85.

Sithole, G., Vosselman, G., 2004. Experimental comparison of filter algorithms for bare-Earth extraction from airborne laser scanning point clouds. *ISPRS J. Photogramm. Remote Sens.* **59**, 85–101.

Smith, M.J., Clark, C.D., 2005. Methods for the visualisation of digital elevation models for landform mapping. *Earth Surface Processes and Landforms* **30**, 885-900.

Sofia, G., Pirotti, F., Tarolli, P., 2013. Variations in multiscale curvature distribution and signatures of LiDAR DTM errors. *Earth Surf. Process. Landforms* **38**, 1116–1134. doi:10.1002/esp.3363

Sofia, G., Marinello, F., Tarolli, P., 2014. A new landscape metric for the identification of terraced sites: The Slope Local Length of Auto-Correlation (SLLAC). *ISPRS J. Photogramm. Remote Sens.* **96**, 123–133. doi:http://dx.doi.org/10.1016/j.isprsjprs.2014.06.018

Sofia, G., Tarolli, P., Cazorzi, F., Dalla Fontana, G., 2015. Downstream hydraulic geometry relationships: Gathering reference reach-scale width values from LiDAR, *Geomorphology*, **250**, 236-248, http://dx.doi.org/10.1016/j.geomorph.2015.09.002.

Swain, C. J. and Kirby, J. F., 2003. The effect of 'noise' on estimates of the elastic thickness of the continental lithosphere by the coherence method. *Geophys. Res. Lett.* **30**, 1574.

Sweeny, K. E., Roering, J. J., Ellis. C., 2015. Experimental evidence for hillslope control of landscape scale. *Science*, **349**(6243), 51-53.

Tarolli, P., Tarboton, D.G., 2006. A New Method for Determination of Most Likely Landslide Initiation Points and the Evaluation of Digital Terrain Model Scale in Terrain Stability Mapping. *Hydrology and Earth System Sciences* **10**: 663-677.

Tarolli, P. and Dalla Fontana, G., 2009. Hillslope-to-valley transition morphology: New opportunities from high resolution DTMs. *Geomorphology* **113**, 47–56.

Tarolli, P., Sofia, G., Calligaro, S., Prosdocimi, M., Preti, F., Dalla Fontana, G. 2015. Vineyards in terraced landscapes: New opportunities from LIDAR data. *Land Degrad. Develop.*, **26**, 92-102.

784 Tate N. J., 1998. Estimating the fractal dimension of synthetic topographic surfaces.
785 *Computers and Geosciences* **24**, 325-334.
786
787 Tate, N. J., 1998. Maximum entropy spectral analysis for the estimation of fractals in
788 topography. *Earth Surface Processes and Landforms* **23**, 1197-1217.
789
790 Tomkin, J. H., 2009. Numerically simulating alpine landscapes: The geomorphological
791 consequences of incorporating glacial erosion in surface process models.
792 *Geomorphology* **103**, 180-188.
793
794 Tseng, C.-M., Lin, C.-W., Dalla Fontana, G., Tarolli, P., 2015. The topographic signature
795 of a major typhoon. *Earth Surf. Processes and Landforms*. doi:10.1002/esp.3708
796
797 Tucker, G.E., Lancaster, S.T., Gasparini, N., Bras, R.L., 2001. The channel-hillslope
798 integrated landscape development (child) model. In: Harmon, R., Doe, W. (Eds.),
799 *Landscape Erosion and Evolution Modeling*, iii ed., Kluwer Academic/ Plenum
800 Publishers, New York, pp. 349–388.
801
802 Tucker, G., Hancock, G. R., 2010. Modelling landscape evolution. *Earth Surface*
803 *Processes and Landforms* **35**, 28-50.
804
805 Van der Mark, C. F., Blom, A., Hulscher S. J. M. H., 2008. Quantification of variability in
806 bedform geometry, *J. Geophys. Res.,* **113**, F03020, doi:10.1029/2007JF000940.
807
808 Venditti, J.G., 2012. Bedforms in sand-bedded rivers. In: Shroder, J., Jr., Wohl, E.
809 (Eds.), *Treatise on Geomorphology*. Academic Press, San Diego, CA, **9**, 137-162.
810
811 Wechsler SP, Kroll C., 2006. Quantifying DEM uncertainty and its effect on topographic
812 parameters. *Photogrammetric Engineering and Remote Sensing* **72**, 1081–1090.
813
814 Weissel, J. K., Pratson, L. F., Malinverno, A., 1994. The length-scaling properties of
815 topography. *J. Geophys. Res*. **99**, 13997-14012.
816
817 Wessel, P., 1998. An Empirical Method for Optimal Robust Regional-Residual
818 Separation of Geophysical Data*. Mathematical Geology* **30**, 391-408.
819
820 Wessel, P. & Smith, W. H. F., 1998. New, improved version of Generic Mapping Tools
821 released. *Eos Trans. Am. Geophys. Union* **79**, 579.
822
823 Wessel, P., 2001. Global Distribution of Seamounts Inferred from Gridded Geosat/ERS-
824 1 Altimetry. *J. Geophys. Res.* **106**, 19431–19441.
825
826 Willgoose, G.R., Bras, R.L., Rodriguez-Iturbe, I., 1991. A physically based coupled
827 network growth and hillslope evolution model, 1, theory. *Water Resources Research* **27**,
828 1671–1684.
829
830 Willgoose, G., 1994. A physical explanation for an observed area-slope-elevation
831 relationship for catchments with declining relief, *Water Resour. Res.,* **30**(2), 151–159,
832 doi:10.1029/93WR01810
833
834 Wohl, E., 2004. Limits of downstream hydraulic geometry. *Geol.* **32**, 897–900.
835 doi:10.1130/G20738.1
836

Wren, E. A., 1973. Trend Surface Analysis – A review. *Canadian Journal of Exploration Geophysics* **9**(1), 39-45.

Zhang, D., Narteau, C. & Rozier, O., 2010. Morphodynamics of barchan and transverse dunes using a cellular automaton model. *J. Geophys. Res.* **115**, F03041.

Zhou, Q., Liu, X., 2002. Error assessment of grid-based flow routing algorithms used in hydrological models. *Int. J. Geogr. Inf. Sci.* **16**, 819–842. doi:10.1080/13658810210149425

Zhou, Q. M. and Liu, X. J., 2004. Analysis of errors of derived slope an aspect related to DEM data properties. *Computers and Geosciences* **30**, 369-378.

Zhou, Q., Liu, X., 2008. Assessing Uncertainties in Derived Slope and Aspect from a Grid DEM, in: Zhou, Q., Lees, B., Tang, G. (Eds.), Advances in Digital Terrain Analysis SE - 15, *Lecture Notes in Geoinformation and Cartography*. Springer Berlin Heidelberg, pp. 279–306. doi:10.1007/978-3-540-77800-4_15

Figures

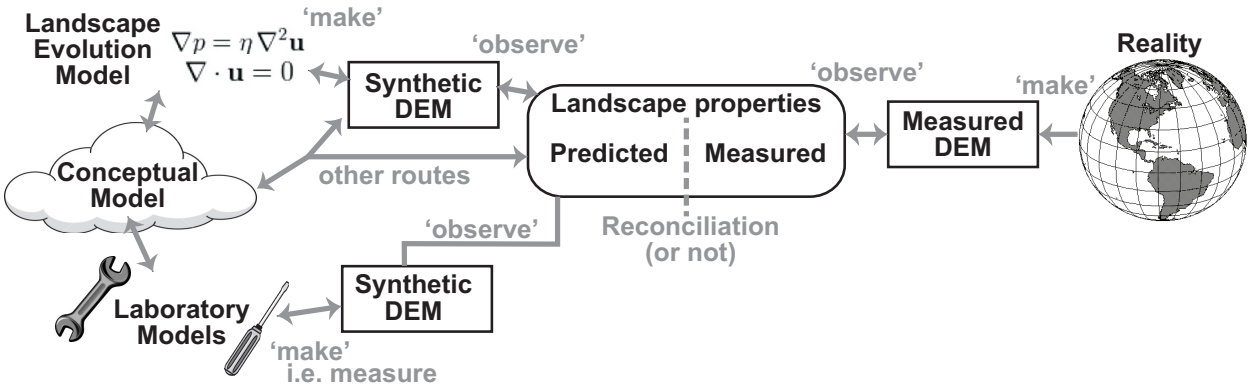

Fig 1: Illustration of the pathways and stages in reconciling geomorphological models with reality in order to understand the physical processes that sculpt planetary surfaces. Stages are in black, and tasks undertaken to move between them are in grey, with double-headed arrows indicating possible feedbacks. Synthetic DEMs may be created through various routes, and may be employed to add rigor to both the making of DEMs and the observing of them to derive landscape properties.

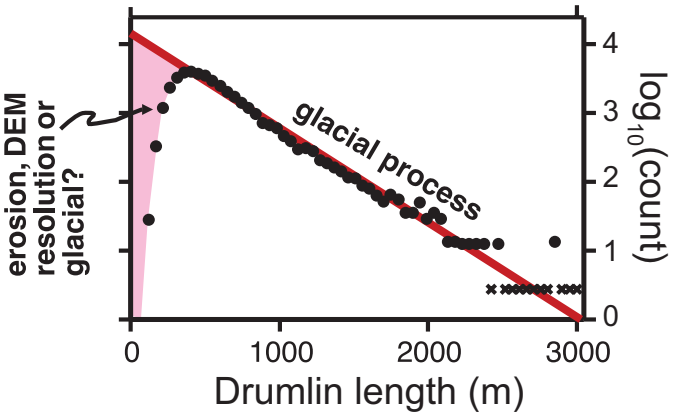

Fig. 2: Semi-logarithmic frequency plot of the lengths, *L*, of UK drumlins adapted from Hillier et al. [2013]. Black dots are data digitised from Fig. 8 of Clark et al. [2009], with a bin width of ~50 m. Red line is the exponential trend. Crosses indicate zero counts, placed at a nominal value of 1. Aspects of the curve are speculatively associated with processes, glacial or related to erosion and DEM construction.

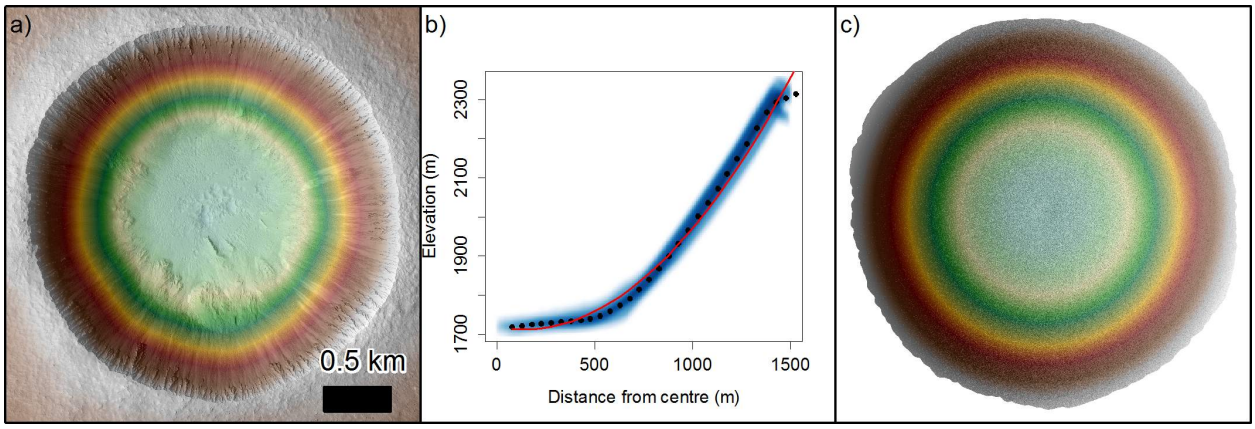

875

876 **Fig. 3**: a) HiRISE image of Zumba crater on Mars coloured according to elevation;
877 HiRISE image DT2EA_002118_1510_003608_1510_A01 and DEM
878 DTEEC_002118_1510_003608_1510_A01, credit NASA/JPL/UofA. b) Radial elevation
879 profile; blue shading illustrates the data distribution, black dots are averages within 50 m
880 distance bins, and the red line is a parabolic fit to those points. c) A synthetic crater
881 created by rotating the parabolic equation, overlain by uncorrelated Gaussian noise and
882 displayed as in a).

883

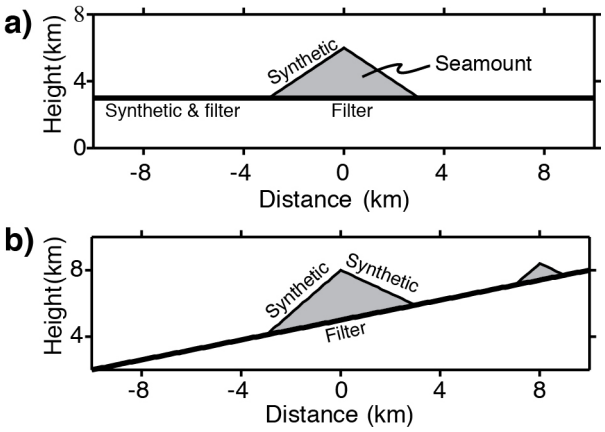

884

885 **Fig. 4:** a) A simple 2D (i.e., distance-height profile) synthetic seamount (grey shading)
886 [Hillier, 2008], which following Kim & Wessel [2008] is conical with a radius of 3 km and
887 summit height of 3 km above the surrounding seafloor. The thin black line is the
888 synthetic topography, and the thick black line the filter's output b) A more demanding
889 test of two, variably sized seamounts upon a sloping surface.

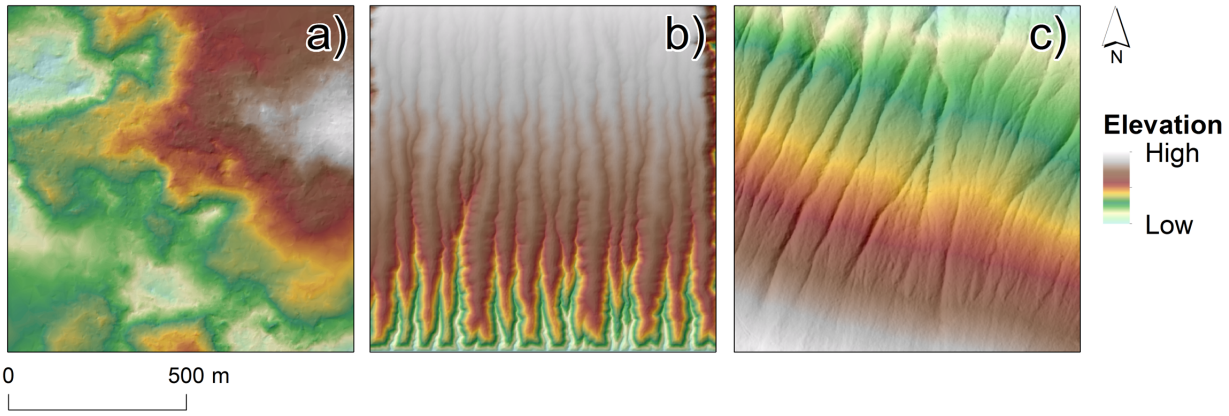

Fig 5. Comparison of simulated DEMs in a) and b) with LiDAR measurement of a real landscape in the South of Italy in c). a) Fractional Brownian motion [Mandelbrot, 1983]; initial roughness of the surface = 0.2, initial elevation of the surface = 0.0, and change of roughness over change of terrain = 0.005. Output is dimensionless, but is effectively given the same scale and resolution as c) by assigning each pixel a 2x2 m size. b) A landscape model [Refice et al. 2012] that evolves through time a southward-dipping initial topography containing small-scale randomness, with all 4 boundaries closed except lower right corner. Simulated time is ~30 kyr and the run parameters are: tectonic uplift u_f = 1 mm/yr; diffusivity constant k_d = 0.2 m^2/yr; with channelling parameters of $K_c = 10^{-4}$ $m^{(1-2m)}$/yr, m = 0.5, and n = 1. The spatial dimensions of b) are as in c). Centroid in c) is 14°37'59.46"E, 40°43'25.80"N.

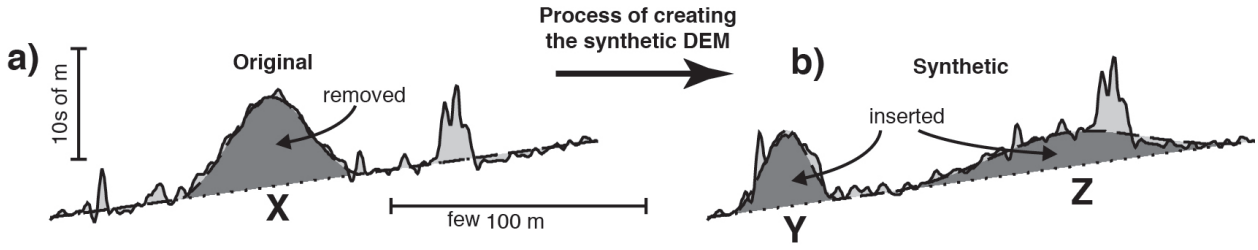

Fig. 6: Idealised distance-height profiles to illustrate the process used by Hillier and Smith [2012] to create synthetic DEMs. There are three 'components'. Drumlins, that are shaded dark grey, rise above a regional trend indicated by a dotted line. These are overprinted by 'clutter' or 'noise' shown in light grey. a) In the process the upper and lower surfaces of the drumlin (X) are estimated to define it, and its height is subtracted from the measured DEM. b) Two Gaussian shaped drumlins (Y and Z) are then inserted by adding their height to create the synthetic DEM.

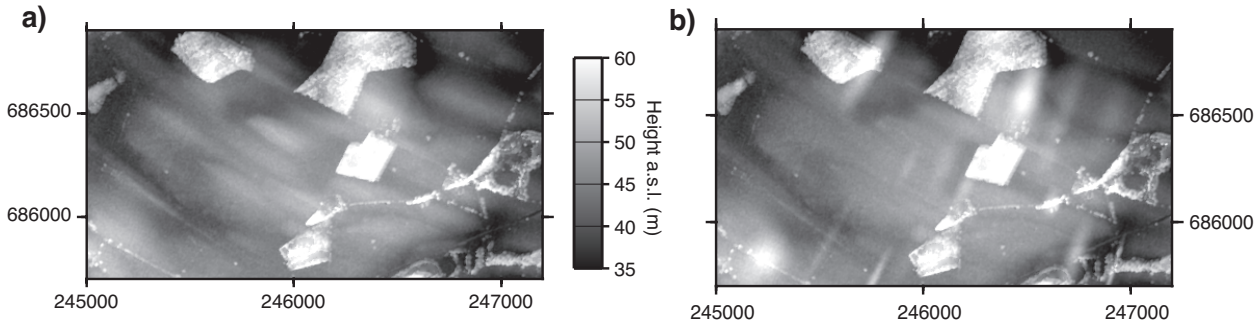

912

913 **Fig. 7:** Illustration of a real DEM in a) and a 'hybrid' synthetic generated from it. Method
914 used is as in Fig. 6 [Hillier and Smith, 2012], adapted to locally align drumlins with each
915 other [Hillier et al., 2014]. Map coordinates are of the British National Grid (5 m grid).
916 Synthetic drumlins were orientated at 90 degrees to the original to avoid any possible
917 confusion with any incompletely removed original ice flow fabric during the mapping
918 exercise.

919